MATEC Web of Conferences **286**, 07006 (2019) https://doi.org/10.1051/matecconf/201928607006
CMM2019

Reducing drag on a flat plate subjected to incompressible laminar flow

A. AGRISS[1,*] , M. AGOUZOUL[1,] , A. ETTAOUIL[1,***]**

[1]Mohammed V University-Rabat, Mohammadia School of Engineers, Avenue Ibn Sina, P.O. Box 765-Agdal, Rabat, Morocco
Mechanical and Energetic Engineering Research Team: Modeling and Experimentation ERG2(ME)
email addresses: *amineagriss@gmail.com, **m.agouzoul@gmail.com, ***ettaouil.ab@gmail.com

Abstract :

The idea behind this work comes from the question: What is the impact of plate corrugations on drag? In this context, a numerical study of laminar incompressible flow over a flat plate and over corrugated plates is carried out. Numerical analysis is performed for low Reynolds numbers (Re= 10, Re = 50, Re = 100, Re = 500, Re =1000) using the computational fluid dynamics (CFD) software ANSYS FLUENT. Simulations results are compared to each others and with those of the reference plate (flat plate (figure 4a)). Comparisons are made via drag coefficient C_d. This work is the beginning of a study that evaluates the impact of corrugations on drag reduction on a flat plate.

Keywords : *drag, ANSYS FLUENT, flat plate, corrugated plate, laminar, flow*

1 Introduction

Drag reduction is a very interesting topic thanks to the gain of energy that it allows. Several drag reduction techniques have been suggested by researchers in several fields (aeronautics, automotive ...).

In that sense, adding agents to fluid, especially polymers, is a good solution to reduce drag. Then, surfactants with their four types (anionic, cationic, nonionic and amphoteric) are also good drag reducers [1].

Other solutions have been proposed by adding drag reducers such as devices added at wingtips of an aircraft (flyers, flaps ...). These devices act on marginal vortices to reduce drag [2].

In addition, there are several boundary layer control methods that have been developed to reduce frictional resistance of streamlined bodies, such as the injection of a different gas [3], the acceleration of the boundary layer [4], etc. All these devices are described in detail in scientific literature.

Finally, the use of a liquid film on the surface of a body reduces its frictional resistance [5].

In this study, drag reduction is achieved by changing the shape of a flat plate in laminar flow regime. Simulations are performed by the use of the CFD software ANSYS FLUENT. This work is a preliminary study that assesses the influence of corrugations (shapes and orientations) and other patterns on drag force exerted on the plate.

2 Numerical modeling

This work deals with the study of a laminar incompressible fluid flow on a plate (dimensions: $1\mathrm{m}\times1\mathrm{m}$) (figure 3).

The fluid (air) has a density ρ ($\mathrm{kg\,m^{-3}}$), a kinematic viscosity ν ($\mathrm{m^2\,s^{-1}}$) and a pressure p (Pa).

Non Dimensionalized Navier-Stokes equations in Cartesian coordinates for an incompressible fluid are:

$$\frac{\partial \mathbf{V}}{\partial t} + (\mathbf{V}.\nabla)\mathbf{V} = -\mathbf{gradp} + \frac{1}{Re}\nabla^2\mathbf{V} \qquad (1)$$

In these equations, variables are non-dimensionalized by choosing the reference scales $L = 1\mathrm{m}$ and $U = 1\mathrm{m/s}$.

Where L is the length of the flat plate and U is the fluid freestream velocity.

The Reynolds number is defined by:

$$Re = \frac{UL}{\nu} \qquad (2)$$

The drag coefficient is defined by:

$$C_d = \frac{F_t}{\frac{1}{2}\rho U^2 S} \qquad (3)$$

where F_t is the drag force and S is the surface area of the plate.

3 Tests configuration

The figure 1 represents the boundary conditions for the various tests. These conditions are detailed in the figure 2.

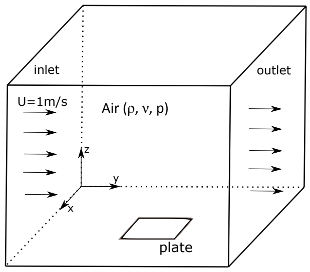

Figure 1: *Boundary conditions of simulations*

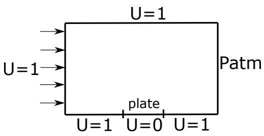

(a) *Front view*

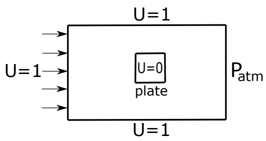

(b) *Top view*

Figure 2: *Boundary conditions description*

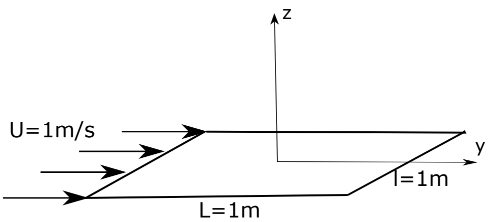

Figure 3: *Flat plate exposed to airflow*

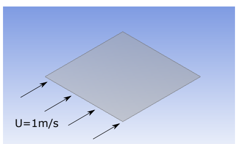

(a) *Reference plate*

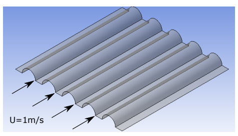

(b) *Corrugated plate*

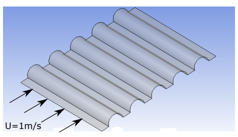

(c) *Inverted corrugated plate*

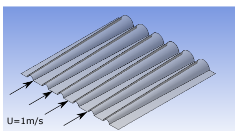

(d) *Convergent corrugated plate*

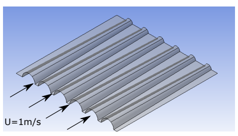

(e) *Divergent corrugated plate*

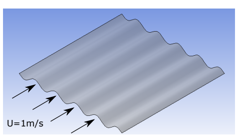

(f) *Sinusoidal plate*

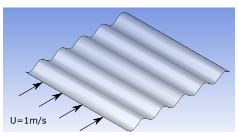

(g) *Inverted sinusoidal plate*

Figure 4: *The studied shapes of the plate*

Simulations are realized in steady state, with a calculation precision of 10^{-6} and their purpose is the determination of drag coefficient C_d for each of the plate shapes.

4 Results and discussion

The figure 4 represents the studied shapes of the plate. They have the same dimensions ($1\text{m}\times 1\text{m}$) and they are subject to the same flow conditions and for which drag coefficient C_d is calculated.
The corrugated plate (4b) and the inversed corrugated plate (4c) are identical but their flow directions are different. Similarly for the convergent corrugated plate (4d) and the divergent corrugated plate (4e). As well as for the sinusoidal plate (4f) and the inverted sinusoidal plate (4g).
Tables 1, 2 and 3 represent drag coefficients C_d and the relative drag modifications $\frac{\Delta C_d}{C_d}$ versus the reference plate (4a) obtained for the studied shapes and for the various Reynolds numbers.

Table 1: *Drag coefficient C_d of the reference plate compared to corrugated and inverted corrugated plates*

Re	4a	4b		4c	
	C_d	C_d	$\frac{\Delta C_d}{C_d}$	C_d	$\frac{\Delta C_d}{C_d}$
10	2.305	3.048	32.2%	4.002	73.6%
50	0.562	0.725	33.8%	0.996	77.2%
100	0.325	0.415	27.7%	0.609	87.4%
500	0.105	0.132	25.7%	0.248	136.2%
1000	0.068	0.085	25%	0.182	167.6%

Table 2: *Drag coefficient C_d of the reference plate compared to convergent corrugated and divergent corrugated plates*

Re	4a	4d		4e	
	C_d	C_d	$\frac{\Delta C_d}{C_d}$	C_d	$\frac{\Delta C_d}{C_d}$
10	2.305	3.294	42.9%	3.391	47.2%
50	0.562	0.780	38.8%	0.776	38.1%
100	0.325	0.445	36.9%	0.432	32.9%
500	0.105	0.141	34.3%	0.127	21%
1000	0.068	0.092	35.3%	0.079	11%

Table 3: *Drag coefficient C_d of the reference plate compared to sinusoidal and inverted sinusoidal plates*

Re	4a	4f		4g	
	C_d	C_d	$\frac{\Delta C_d}{C_d}$	C_d	$\frac{\Delta C_d}{C_d}$
10	2.305	2.977	29.2%	2.071	−10.2%
50	0.562	0.703	25.1%	0.527	−6.2%
100	0.325	0.399	22.7%	0.314	−3.4%
500	0.105	0.123	17.1%	0.107	1.9%
1000	0.068	0.078	14.7%	0.070	2.9%

As expected, drag coefficient C_d is inversely proportional to Reynolds number Re for all configurations of the plate. This is consistent with several existing formulas in the literature that express drag coefficient as a function of Reynolds of flow.
The inverted corrugated plate (4c) is the most unfavorable configuration. It increases hugely C_d of the flat plate for all Reynolds numbers especially for Re=500 (increase of 136.2% for Re=500). That's why it's necessary to avoid such configurations in low Reynolds number designs.
Concerning the corrugated plate (4b), the convergent corrugated plate (4d) and divergent corrugated plate (4e), they always increase drag coefficient with respect to the flat plate (4a).
When Reynolds number increases, C_d of the divergent corrugated plate (4e) decreases compared to the convergent corrugated plate (4d) and compared to the corrugated plate (4b) (for Re=1000, C_d of the divergent corrugated plate increase by 11%, C_d of the convergent corrugated plate increase by 35.3% and C_d of the corrugated plate increase by 25% compared to the flat plate). This result shows that divergent corrugations improve C_d of simple and convergent corrugations.
The sinusoidal configuration (4f) has the lowest C_d of all configurations (4b, 4c, 4d and 4e), but its C_d remains higher than the C_d of the flat plate (4a).
Finally, the inverted sinusoidal plate (4g) is the configuration that reduces drag coefficient of the flat plate. In fact, for low Reynolds numbers, the reduction of C_d is outstanding:

- For Re=10, the inverted sinusoidal plate reduces remarkably drag coefficient of the flat plate C_d from 2.305 to 2.071 (reduction of 10.2%).
- For Re=50, this sinusoidal plate reduces drag coefficient C_d from 0,562 to 0,527 (reduction of 6.2%).
- For Re=100, it reduces it from 0,325 to 0,314 (reduction of 3.4%).
- For the Reynolds numbers Re=500 and Re=1000, a slight increase of C_d is observed compared to the flat plate.

This configuration will be used mainly for low Reynolds numbers since it reduces remarkably C_d by 10.2% for Re=10, by 6.2% for Re=50 and by 3.4% for Re=100.

5 Conclusion

In this preliminary work, numerical simulations were carried out to study the effect of changing plate shape on drag reduction for a laminar incompressible air flow on this plate.
Simulations were performed by the CFD software ANSYS FLUENT.
Drag coefficients are compared between the various plate shapes. The analysis of results leads to conclude that the inverted sinusoidal plate reduces drag coefficient of the plate for low Reynolds numbers.
Future works will focus on the optimisation of flat plate shape to reduce drag coefficient for high Reynolds number flows and the extension to turbulent flows.

References

[1] F. Hadri, *Contribution à l'étude de la réduction de la traînée en écoulement turbulent d'une solution de CTAC*, Ph.D. Dissertation, University of Caen, 2008.

[2] R.V.J. Viard, *Dispositifs fluidiques de Contrôle actif d'écoulements à base de Microsystèmes Magnéto-Electro-Mécaniques (MMEMS) (conception, réalisation, tests)*, Ph.D. Dissertation, Ecole Centrale in Lille, 2010.

[3] S.A. Mäkiharju, S.L. Ceccio, *On multi-point gas injection to form an air layer for frictional drag reduction*, Ocean Eng. 147 (2018) 206 – 214.

[4] K. Gersten, H. Schlichting, *Boundary-LayerTheory Ninth Edition*, Springer-Verlag, Berlin Heidelberg, Germany, 2017.

[5] N. Klyuev, Y. Kryukov, A. Gimadiev, *Reducing friction drag on flat plates*, Procedia Engineering 176 (2017) 661 – 668.